Grid Resolution and Solution Convergence For Mars Pathfinder Forebody

Heather L. Nettelhorst and Robert A. Mitcheltree
NASA Langley Research Center
Hampton, VA 23681-0001

Introduction

As part of the Discovery Program, NASA plans to launch a series of probes to Mars. The Mars Pathfinder project[1] is the first of this series with a scheduled Mars arrival in July 1997. The entry vehicle will perform a direct entry into the atmosphere and deliver a lander to the surface. Predicting the entry vehicle's flight performance and designing the forebody heatshield requires knowledge of the expected aerothermodynamic environment. Much of this knowledge can be obtained through computational fluid dynamic (CFD) analysis.

The accuracy of CFD analysis, however, is influenced by many factors. In particular, it is necessary to discretize the physical domain into a grid with sufficient resolution to capture the relevant physics. In preforming this task, it is also important to consider the computational cost of a flowfield solution. The computational time required to generate a CFD solution varies as the number of grid cells squared. A desirable grid, therefore, is one which resolves the flowfield using the fewest number of grid cells. The first objective of the present work is to examine grid resolution requirements for the Mars Pathfinder forebody. In addition, the solution must be converged. This requires the numerical algorithm to be iterated until the solution's associated residual error becomes zero. In practice, driving the residual to zero is unnecessary. Therefore, the second objective is to establish the degree of solution convergence necessary to predict accurate surface pressures and convective heating.

The CFD tool used in this study is the Langley Aerothermodynamic Upwind Relaxation Algorithm (LAURA)[2-3] computer code developed by P. A. Gnoffo. It is an upwind-biased, point-implicit scheme for solving the Navier-Stokes equations in thermochemical nonequilibrium hypersonic flow. Explicit instructions on the use of the LAURA code for air can be found in the user's manual[4]. In order to simulate Pathfinder's entry into Mars, the gas kinetics of air are substituted with those of the predominatly CO_2 atmosphere of Mars[5-6]. Appendix A contains user information to run the Mars atmosphere version of LAURA.

The Mars Pathfinder entry vehicle is similar to that of the Viking probes. It is a spherically-blunted cone with half angle of 70^0 . Pathfinder's nose radius is 0.6625 m and the shoulder radius is 0.06625m. The overall vehicle diameter is 2.65 m compared with 3.5 m for Viking. One half of the axisymmetric forebody profile and a typical computational mesh is shown in Fig. 1.

Two important quantities associated with Pathfinder's entry are the expected maximum heating and the vehicle's drag coefficient. Based on a vehicle ballistic coefficient of 55 kg/m^2 and a 7.65 km/sec ballistic entry at -14.2 degrees, the vehicle's trajectory is predicted to encounter maximum convective heating at 40.7 km altitude and 6592 m/sec velocity. At this altitude, the density and

temperature of the CO_2-N_2 atmosphere are 3.24e-04 kg/m^3 and 162 K. Solutions from the grid resolution study and the convergence study for the Pathfinder geometry at this trajectory point are presented in the *Results* section. All results are laminar, axisymmetric solutions to the thin-layer Navier-Stokes equations. The wall boundary conditions specify wall temperature to be 2000 K which is approximately the radiative equilibrium value for the expected heating levels. Species mass fractions at the wall are set to their freestream values.

Grid Resolution

Grid requirements differ based on the geometry examined and the CFD tool employed. This discussion pertains to LAURA solutions on blunt bodies.

As stated previously, grid resolution depends on discretization of the physical domain. To accurately capture flowfield phenomena, the physical domain's discretization must be based on flowfield gradients. Typically regions of steep flowfield gradients, i.e., at the shock and near the wall, require finer grid resolution. A gradient-dependent quantity such as surface heating is most sensitive to grid resolution near the wall[7]. Grid resolution near the the wall must be adequate to capture the physical processes of viscous diffusion, mass diffusion, and thermal conduction. For Mars Pathfinder's entry flowfields, where local Prandtl and Lewis numbers are of order one[5], this requirement is met if the cell Reynolds number is of order one. Cell Reynolds number is defined as;

$$Re_c = \frac{\rho a \Delta\eta}{\mu} \tag{1}$$

Where ρ is the local density, a is the local speed of sound, $\Delta\eta$ is the height of the 1st cell off the wall, and μ is the local viscosity. Experience has shown that the Re_c requirement need only be met for cells adjacent to the wall. As the distance from the wall increases, cell size can increase but is constrained by a maximum growth factor and cell size. LAURA contains grid adaption capabilities which redistribute grid cells near the wall. This redistribution depends on two code inputs: (1) cell Reynolds number, Re_c , described above and (2) f_{str}. f_{str} is the fraction of normal body cells included in the stretching region[7]. The stretching region is about the thickness of the boundary layer. The cells beyond the stretching region are constant in size. A complete description of the boundary-layer grid adaptation appears in the LAURA user's Manual[4].

Grid Resolution Results

Initially the grid study examined four grids with the default settings for Re_c and f_{str} of 1.0 and 0.5 while varying the number of cells normal to the body. Table 1 lists the first four grids examined.

Table 1 - Initial Grid Study

grid	$Cell_{parallel}$	$Cell_{normal}$
1	38	64
2	38	80
3	38	128
4	38	160

A grid's ability to resolve the flowfield is evaluated based on its prediction of surface pressure and convective heating. Comparison of the surface pressures and integrated drag coefficients for

grids 1-4 is shown in Fig. 2. The figure shows the predicted pressure distributions are in close agreement. The drag coefficients agree within 0.3%. Based on this figure, grid 1 is adequate to predict surface pressure and drag coefficient. For this high velocity flowfield, viscous drag is small.

Figure 3 presents the surface heating for the same four grids. As expected, the surface heating prediction is more sensitive to grid resolution. As the number of cells normal to the body is increased from 64 to 80 to 128, the heating prediction on the conical section decreases. Further increasing the number of cells normal to the wall to 160 results in only a small improvement in the heating predition. Based on Fig. 3., grid 3 with 38 cells along the body and 128 cells normal to the body might be judged an acceptable trade-off between sufficient grid resolution and computational cost.

Grids 1-4 use the default choices of 1.0 and 0.5 for Re_c and f_{str}. To reduce the computational cost of the calculations, variations in these inputs on 38 x 64 grids are examined next to determine if a 38 x 64 grid can be found that produces acceptable heating predictions. Table 2 presents the variations examined.

Table 2 - 38 x 64 Grid Study

grid	Re_c	f_{str}
5	1.0	0.50
6	2.0	0.50
7	5.0	0.50
8	1.0	0.75
9	2.0	0.75
10	5.0	0.75

Figure 4 demonstrates the effect of varying Re_c on the 38 x 64 grid with $f_{str} = 0.5$ (grids 5-7). The 38 x 128 grid from Fig. 3 is included in the figure as the reference solution. For a grid with 64 points normal to the wall, increasing Re_c improves the heating prediction on the conical section but degrades it at the stagnation point. Figure 5 compares the same variation of Re_c except f_{str} is 0.75. For $f_{str} = 0.75$, increasing Re_c from 1 to 2 improves the heating prediction on the flank without degrading the solution in the nose region. Increasing Re_c to 5 further improves the heating prediction on the flank region but degrades the prediction at the stagnation point. None of the 64-cell grids examined in Figs. 4 and 5 provide heating predictions within acceptable limits of the solution from the 38 x 128 grid. However, if a five percent error due to grid resolution is tolerable, a factor of four reduction in computation times can be realized by using a 64-cell grid. In particular, the choice of f_{str}=0.75 and $Re_c = 2$ produces good stagnation point prediction with only a small error on the vehicle flank. Solution convergence in the next section is illustrated on this grid.

In Figs. 2-5 only variations in the cells normal to the wall have been examined. In Fig. 6., the heating prediction from grids 3 and 9 are compared with that from a 76 x 64 grid with $Re_c = 2$, $f_{str} = 0.75$. This figure illustrates the effect of doubling the number of grid cells parallel to the body. While increasing the grid resolution along the body improves the heating prediction on the vehicle flank, an oscillation appears in the nose region heating. Such oscillations can occur on axisymmetric grids due to the axis singularity along the stagnation line. The axis singularity problem has been documented[8]. Using only 38 cells along the body introduces only small errors in the prediction of surface heating and avoids the complications introduced by the axis singularity.

Solution Convergence Results

A CFD solution is converged when the associated residual error is zero. It is often unnecessary to drive this error to zero. From an engineering standpoint, sufficient convergence occurs when additional iterations of the algorithm will not significantly change the prediction of important solution quantities. For Pathfinder, two important solution quantities are surface pressure and heating. The drag coefficient, C_d, is a single-value indicator of the pressure distribution.

Figure 7 presents the convergence history of C_d for a 32,000 iteration solution for Mars Pathfinder. Appendix B contains details of the examined run which used grid 9 from Table 2. The solid curve in Fig. 7 shows the value of C_d versus iterations. The predicted C_d value at 2500 iterations is within 1 percent of its last computed value, 1.6907. By 9000 iterations, C_d is within 0.1 percent. Typically, the final C_d value is not known and the percent change in C_d is monitored. The dotted curve in Fig.7 represents the percentage change in C_d per 1000 iterations. At 2500 iterations, the percentage change per 1000 iterations is 0.01. When this percentage change is less than 0.001 at 9000 iterations, the value of C_d is within 0.1 percent of its last value. Figure 8 shows the complete pressure distributions at different stages during the first 10000 iterations. There is negligible change in the pressure distribution after iteration 10000.

Figure 9 presents the convergence history of the stagnation point convective heating q_{stag}. Note, the ordinate axis's large range. q_{stag} requires 10000 iterations for the predicted value to be within one percent of the last calculated value 120.76 W/cm^2. By 22000 iterations, it is within 0.1 percent. The percentage change in q_{stag} prediction per 1000 iterations at 10000 iterations, is 0.01. At 20000 iterations, the percentage change has dropped below 0.001. Convergence of the surface heating distribution during the first 10000 iterations is illustrated in Fig. 10. Distributions during the final 22000 iterations are shown in Fig. 11. The overexpansion-recompression region converges last.

Conclusions

As expected, surface convective-heating preditions are more sensitive to near-wall grid resolution than surface pressures. For Re_c= 1 and f_{str}=0.50, a grid of 38 cells along the body and 128 cells normal to the body represents an acceptable trade-off between computational cost and error in predicting surface convective heating. By changing Re_c to 2 and f_{str} to 0.75, a grid of 38 cells along the body and 64 cells normal to the wall is generated which predicts surface heating within 5 percent of those for the 38 x 128 grid while producing a significant reduction in computational cost. Increasing the number of cells along the body from 38 to 76 introduces the axis singularity problem in the near stagnation point heating.

The prediction of convective heating is slower to converge than the surface pressure prediction. For Mars Pathfinder's maximum-heating trajectory point, it requires 9000 iterations for the predicted drag coefficient to be within 0.1 percent of the final value of 1.691. There is negligible change in surface pressure distribution after 10000 iterations. It requires 22000 iterations for the same degree of convergence in the stagnation point convective heating prediction. The final stagnation point heating prediciton is 120.8 W/cm^2. The over-expansion-recompression region just beyond the sphere-cone juncture is the last area of the boundary layer to converge.

When the percentage change in C_d or stagnation point heating is below 0.001 per 1000 iterations, the value predicted for these two quantities in within 0.1 percent of its final value.

References

[1]Hubbard, G. S., Wercinski, P. F., Sarver, G. L., Hanel, R.P., and Ramos, R., "A Mars Environmental Survey (MESUR) - Feasibility of a Low Cost Global Approach," IAF Paper 91-432, Oct. 1991.

[2]Gnoffo, P. A., Gupta, R. N., and Shinn, J. L.," Conservation Equations and Physical Models for Hypersonic Air Flows in Thermal and Chemical Nonequilibrium," NASA TP-2867, Feb. 1989.

[3]Gnoffo, P. A.,"An Upwind-Biased, Point-Implicit Relaxation Algorithm for Viscous, Compressible Perfect-Gas Flows," NASA TP-2953, Feb. 1990.

[4]Cheatwood, F. M., and Gnoffo, P. A.,"A User's Manual for the Langley Aerothermodynamic Upwind Relaxation Algorithm (LAURA)," NASA TM 4674, 1995.

[5]Mitcheltree, R. A., "Aerothermodynamic Methods for a Mars Environmental Survey Mars Entry," *Journal of Spacecraft and Rockets*, Vol. 31, No. 3, May-Jun., 1994, pp. 516-523.

[6]Mitcheltree, R. A., "Wake Flow About a MESUR Mars Entry Vehicle," AIAA Paper 94-1958, Jun. 1994.

[7]Gnoffo, P. A., Hartung, L. C., and Greendyke, R. B., "Heating Analysis for a Lunar Transfer Vehicle at Near-Equilibrium Flow Conditions," AIAA Paper No 93-0270, Jan., 1993.

[8]Grasso, F., and Gnoffo, P. A.,"A Numerical Study of Hypersonic Stagnation Point Heat Transfer Predictions at a Coordinate Singularity," Proceedings of the Eighth GAMM-Conference on Numerical Methods in Fluid Mechanics, Editor Pieter Wesseling, Vol. 29, 1990, pp. 179-188.

Appendix A

The Langley Aerothermodynamic Upwind Relaxation Algorithm (LAURA) User's Manual[4] explains LAURA's installation and operation procedures. These procedures are written for the air version of LAURA. To perform computational analysis of Mars atmosphere entries, several modifications are required to the LAURA code and operating procedures. At present, the Mars modifications are prepared for the LAURA.4.0.5 version.

After LAURA.4.0.5 is installed, the following subroutines must be modified. After each subroutine name, notes are given about the Mars atmosphere modifications. Once these subroutines are in place,. LAURA will run for either air or the Mars atmosphere.

- boundr.F : compile directives are used to disable the finite catalytic air boundary conditions options which apply only to air.
- dirswp.F : in the computation of error norm, a division by internal energy is removed since internal energies for the Mars atmosphere can have value zero.
- kinetic.F : the 14 reaction set for 8 species Mars atmosphere is included.
- mars.F : a substitute for air.f which contains the additional species constants including thermodynamic and transport properties curve fits.
- setup.F : for 8 species Mars atmosphere, set ns0=ns.
- source.F : set vibrational energy removed due to dissociation to ten time the average vibrational energy.
- start.f : include questions for Mars atmosphere options.
- start.format : required for new start.f
- start.inc : required for new start.f
- taskit.F : corrects multitasking error in original LAURA.4.0.5 version.
- thermo.F : include heat-of-formation change for reference temperature change of 0 K to 298.16 K.
- trnsprt.F : vibrational relaxation of CO2 is overwritten with CAMAC data curve fits.

The above subroutines are brought into the local workspace directory. They can be left there or the CUSTOMIZE script file can be used to place the *.F files in the directory LAURA.4.0.5/CUSTOM. Next the PRELUDE command is required which will prompt the user with the appropriate questions to select the Mars atmosphere version. As always, the new code must be compiled with "make" following PRELUDE. A sample INPUTS file to start a Mars Pathfinder run follows.

INPUTS

```
4 nprocs ..... number of processors to be used
2 newjob ..... 0=externally generated, 1=conic, 2=aerobrake
1 ndim ..... flow: 1=axisymmetric, 2=2-D, 3=3-D
1 igovern ..... fluid eqns: 0=Euler, 1=TL N-S, 2=N-S
6592.00 vinfb ..... velocity [m/s]
```

0.324000E-03 rinfb ..... density [kg/m3]
162.000 tinf ..... freestream temperature [K]
0 tempbc . Tw BC: 0=constant, 1=variable, 2=equilibrium radiative
2000.00 twall ..... wall temperature [K]
1 nplanet ..... 0=EARTH, 1=MARS
1 jtype ..... catalytic nature of wall
0 nturb ..... turbulence: 0=no, 1=Cebeci-Smith, 2=Baldwin-Lomax
38 iaq ..... cells in streamwise/axial direction
64 kaq ..... cells in normal direction (maximum)
2 iafe ..... aerobrake geometry option: 0=AFE, 1=sphere, 2=custom
0 iunit ..... 0=m, 1=cm, 2=ft, 3=in, 4=
70.0000 thetaxy ..... body half angle [deg]
70.0000 tau ..... shoulder turning angle [deg]
0.662500E-01 radius ..... shoulder radius [m]
0.662500 rnose ..... nose radius [m]
1.32500 rbase ..... base plane radius [m]

There are additional required modifications to run turbulence, non-constant wall temperatures or finite catalytic boundary conditions.

Due to stiffer chemical kinetics than air, the initial settings in the input file *data* are different for the Mars version. The following table presents a sample *data* history for the above INPUTS files. Each line represents a "run". Variables not listed in this table maintained default values.

nord	itervmx	niterp	iterg	movegrd	maxmoves	errd
1	1	1	200	0	0	0.001
2	1	1	300	0	0	0.001
2	10	10	200	0	0	0.001
2	10	10	300	50	1	0.001
2	10	10	300	50	1	0.001
2	10	10	300	50	1	0.001
2	20	20	500	50	1	0.001
2	20	20	500	50	1	0.001
2	20	20	500	50	1	0.001

Re_c and f_{str}, as discussed in the grid resolution study, are defined in the file *algnshk.vars.strt*

Appendix B

The following table lists the run parameters used to create the *data* presented in the solution convergence study.

Table 1 - Run Log Excerpt

run	nord	itervmx	niterp	iterg	tot iter	mvgrd	maxmv	rfinv	rfivs	CPU time
01	1	1	1	20	20	0	0	2.0	1.0	2.407
02	1	1	1	20	40	0	0	2.0	1.0	2.294
03	1	1	1	20	60	0	0	2.0	1.0	2.164
04	1	1	1	20	80	0	0	2.0	1.0	2.160
05	1	1	1	20	100	0	0	2.0	1.0	2.247
06	1	1	1	50	150	0	0	2.0	1.0	5.654
07	1	1	1	50	200	0	0	2.0	1.0	5.817
08	1	1	1	50	250	0	0	2.0	1.0	5.842
09	1	1	1	50	300	0	0	2.0	1.0	5.905
10	1	1	1	100	400	0	0	2.0	1.0	11.362
11	1	1	1	100	500	0	0	2.0	1.0	22.598
12	2	1	1	100	600	0	0	2.0	1.0	23.999
13	2	10	10	100	700	0	0	2.0	1.0	16.209
14	2	20	20	100	800	100	0	2.0	1.0	23.515
15	2	20	20	100	900	100	0	2.0	1.0	21.862
16	2	20	20	100	1000	100	0	2.0	1.0	21.959
17	2	20	20	100	1100	50	1	2.0	1.0	21.630
18	2	20	20	100	1200	50	1	2.0	1.0	21.474
19	2	20	20	100	1300	50	1	2.0	1.0	21.096
20	2	20	20	100	1400	50	1	2.0	1.0	21.775
21	2	20	20	100	1500	50	1	2.0	1.0	20.753
22	2	20	20	300	1800	100	0	2.0	1.0	61.777
23	2	20	20	300	2100	100	2	2.0	1.0	61.612
24	2	20	20	300	2400	100	0	2.0	1.0	60.702
25	2	20	20	300	2700	100	2	2.0	1.0	61.076
26	2	20	20	300	3000	100	0	2.0	1.0	60.787
27	2	20	20	1000	4000	100	9	2.0	1.0	203.062
28	2	20	20	1000	5000	0	0	2.0	1.0	194.837
29	2	20	20	1000	6000	120	0	2.0	1.0	199.451
30	2	20	20	1000	7000	0	0	2.0	1.0	192.874
31	2	20	20	1000	8000	140	0	2.0	1.0	199.697
32	2	20	20	1000	9000	0	0	2.0	1.0	190.364
33	2	20	20	1000	10000	120	0	1.6	0.6	199.894

Comments: The value of *errd* was set to 0.001 which resulted in grid doubling in runs 11 and 13. The total CPU usage was 1,968 Cray C-90 secs.

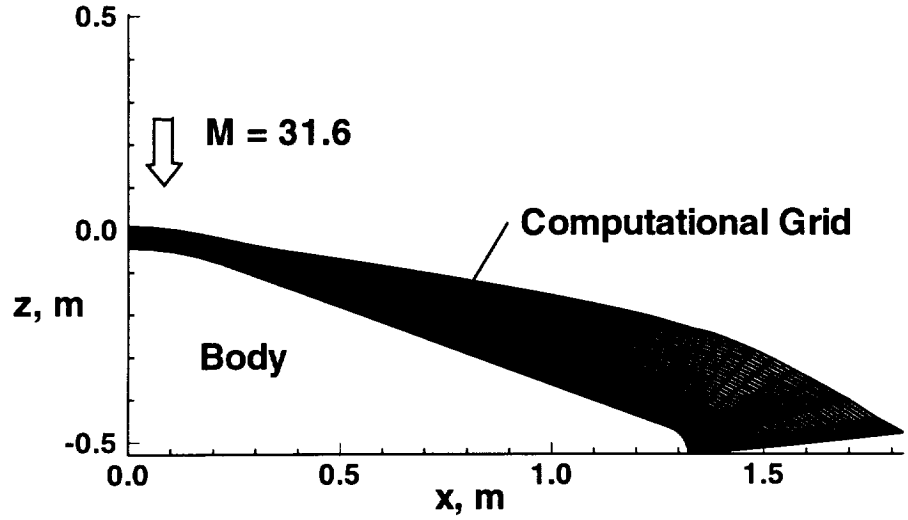

Figure 1: Mars Pathfinder axisymmetric geometry and a 38 x 64 computational mesh.

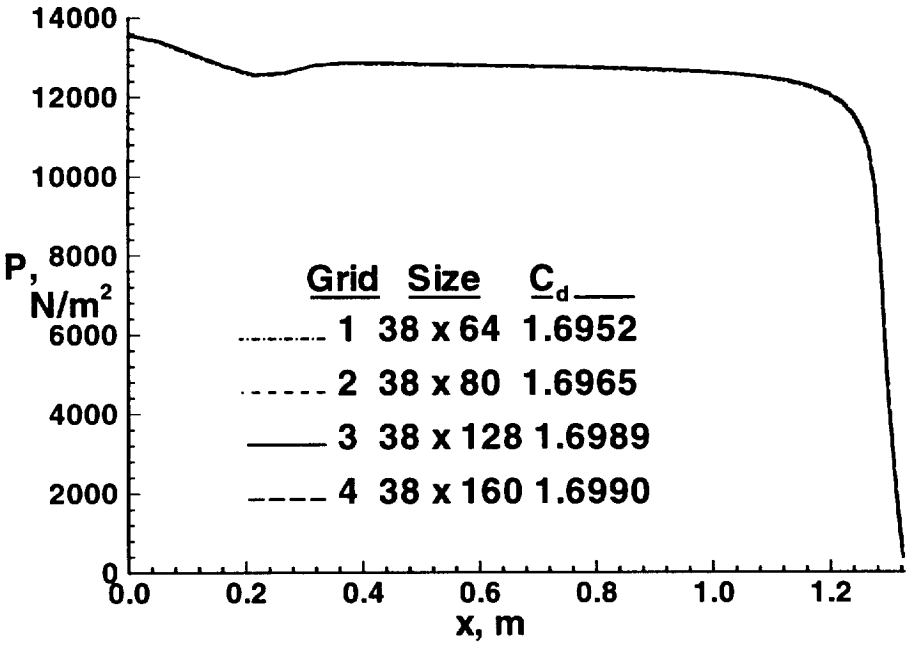

Figure 2: Effect of varying the number of grid cells normal to the wall on surface pressure prediction and drag coefficient.

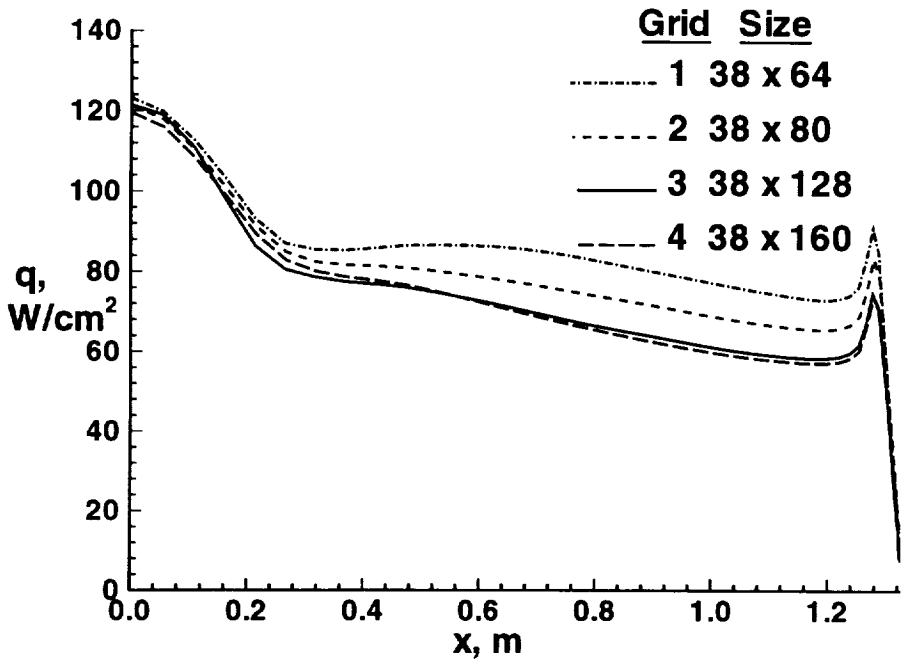

Figure 3: Effect of varying the number of grid cells normal to the wall on surface heating prediction.

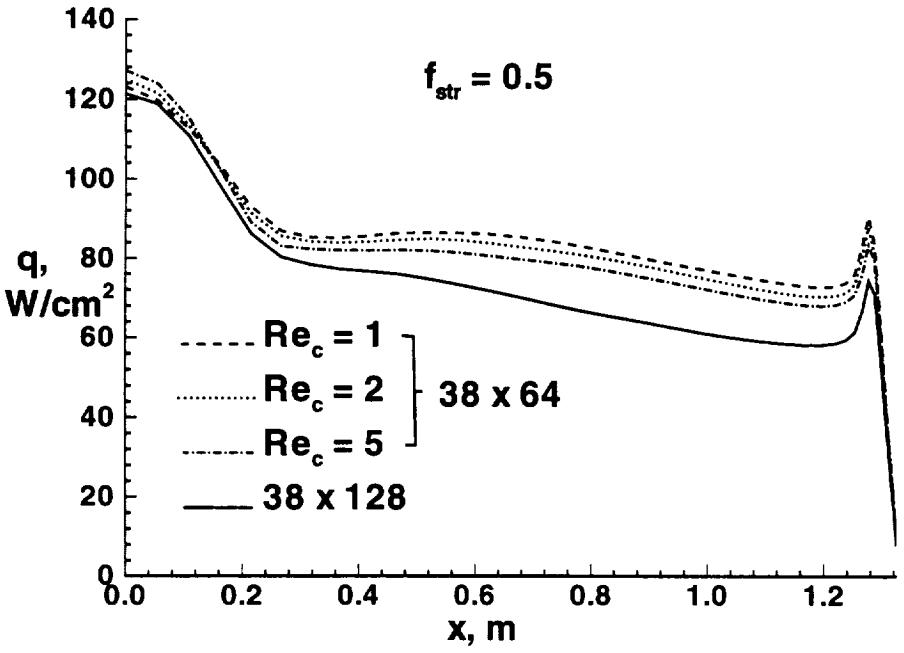

Figure 4: Effect of varying grid stretching parameters on surface heating prediction (38 x 64 grids).

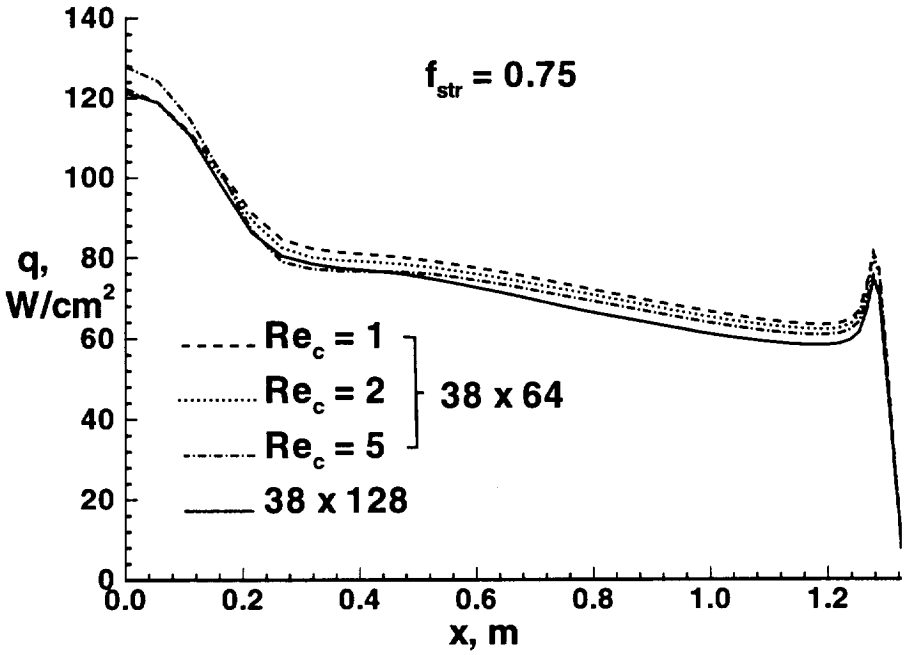

Figure 5: Effect of varying grid stretching parameters on surface heating prediction (38 x 64 grids).

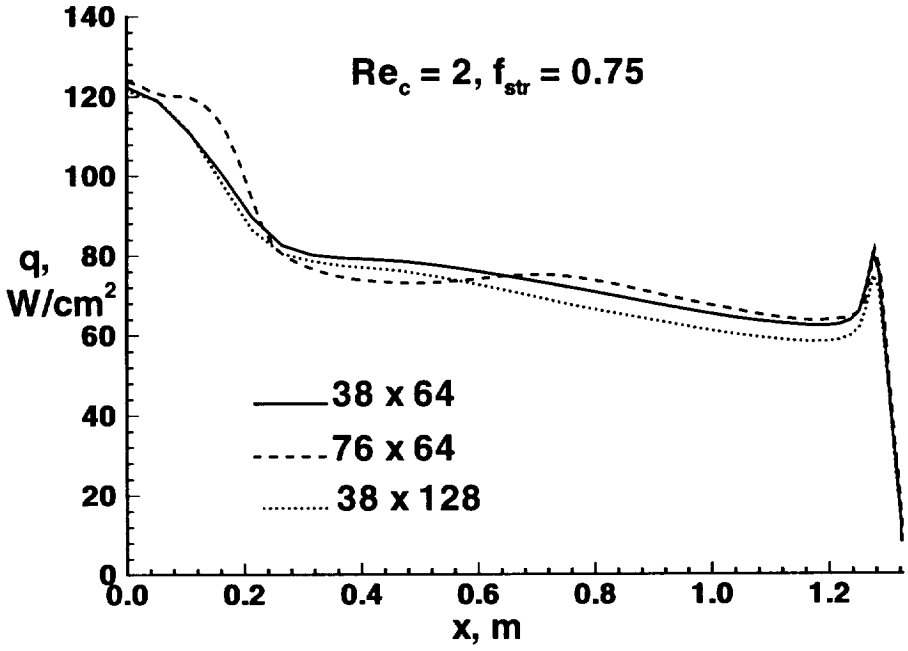

Figure 6: Effect of doubling the number of grid cells along the wall on surface heating prediction.

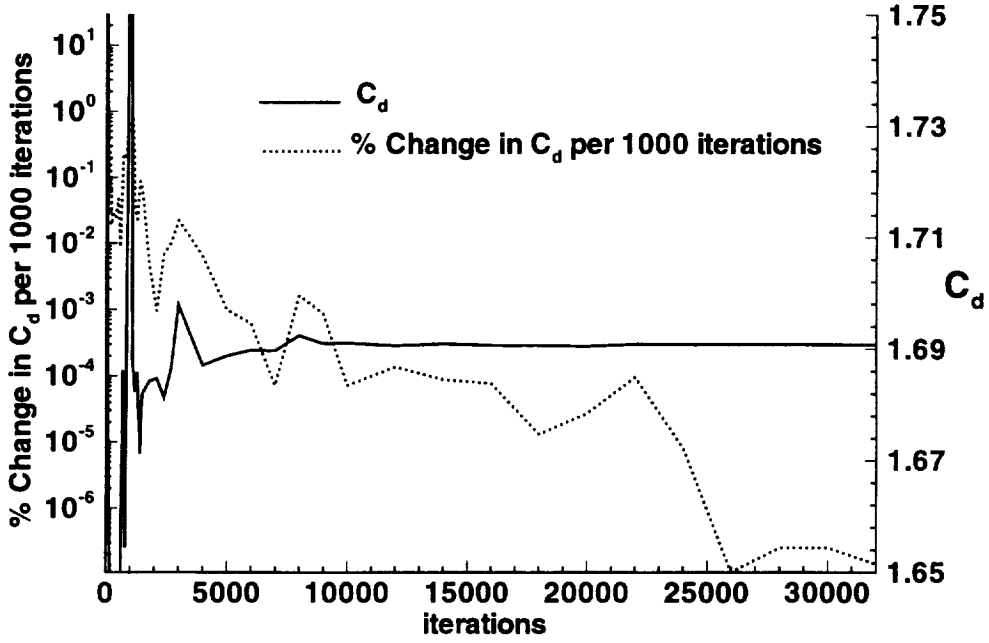

Figure 7: Convergence of the drag coefficient.

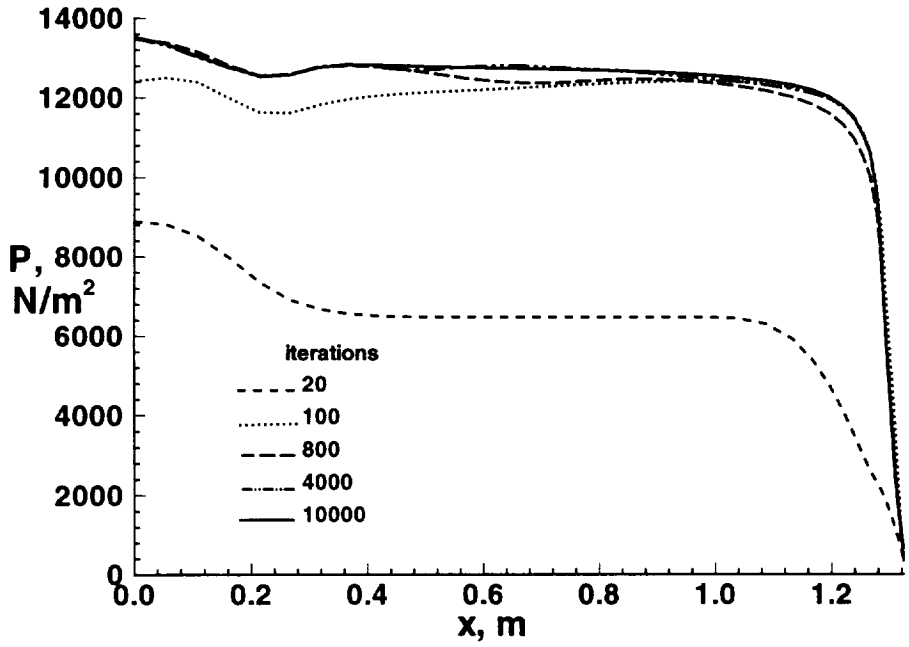

Figure 8: Convergence of surface pressure distribution.

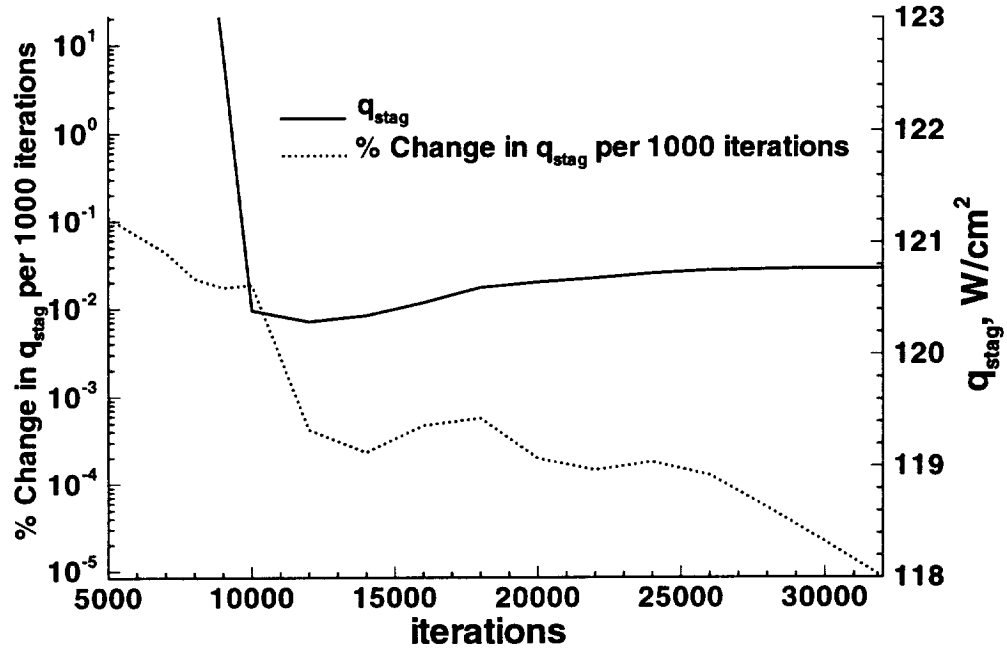

Figure 9: Convergence of Stagnation point heating.

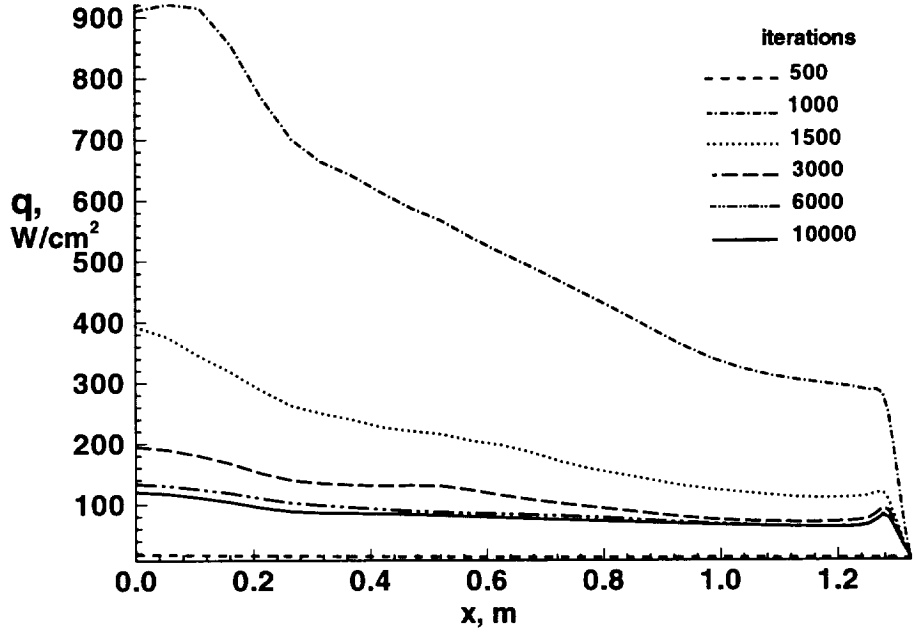

Figure 10: Convergence of surface heating distribution during the first 10000 iterations.

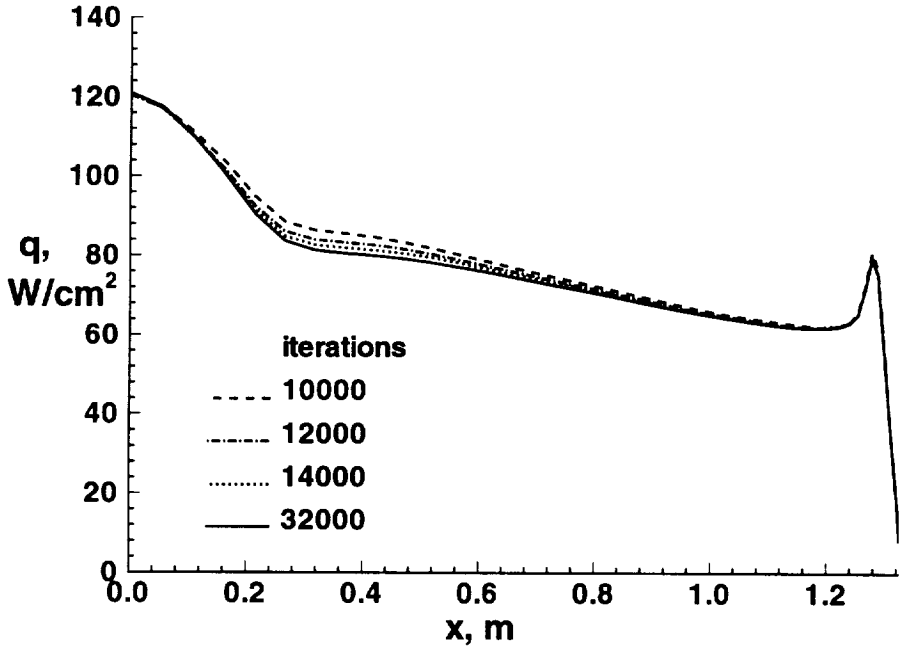

Figure 11: Final convergence of surface heating distribution.

REPORT DOCUMENTATION PAGE

Form Approved
OMB No. 0704-0188

1. AGENCY USE ONLY *(Leave blank)*	2. REPORT DATE	3. REPORT TYPE AND DATES COVERED
	December 1994	Technical Memorandum

4. TITLE AND SUBTITLE
Grid Resolution and Solution Convergence for Mars Pathfinder Forebody

5. FUNDING NUMBERS
WU 242-80-01-01

6. AUTHOR(S)
Heather L. Nettelhorst and Robert A. Mitcheltree

7. PERFORMING ORGANIZATION NAME(S) AND ADDRESS(ES)
NASA Langley Research Center
Hampton, VA 23681-0001

8. PERFORMING ORGANIZATION REPORT NUMBER

9. SPONSORING / MONITORING AGENCY NAME(S) AND ADDRESS(ES)
National Aeronautics and Space Administration
Washington, DC 20546-0001

10. SPONSORING / MONITORING AGENCY REPORT NUMBER
NASA TM-109173

11. SUPPLEMENTARY NOTES
Heather L. Nettelhorst and Robert A. Mitcheltree: Langley Research Center, Hampton, VA.

12a. DISTRIBUTION / AVAILABILITY STATEMENT
Unclssified-Unlimited

Subject Category 64

12b. DISTRIBUTION CODE

13. ABSTRACT ***(Maximum 200 words)***

As part of the Discovery Program, NASA Plans to launch a series of probes to Mars. The Mars Pathfinder project is the first of this series with a scheduled Mars arrival in July 1997. The entry vehicle will perform a direct entry into the atmosphere and deliver a lander to the surface. Predicting the entry vehicle's flight performance and designing the forebody heatshield requires knowledge of the expected aerothermodynamic environment. Much of this knowledge can be obtained through computational fluid dynamic (CFD) analysis.

14. SUBJECT TERMS
computational fluid dynamic, Langley Aerothermodynamic Upwind Relaxation Algorithm (LAURA), and pathfinder

15. NUMBER OF PAGES
15

16. PRICE CODE
A03

17. SECURITY CLASSIFICATION OF REPORT	18. SECURITY CLASSIFICATION OF THIS PAGE	19. SECURITY CLASSIFICATION OF ABSTRACT	20. LIMITATION OF ABSTRACT
Unclassified	Unclassified	Unclassified	